J Mol Model (2013) 19:2173–2181
DOI 10.1007/s00894-013-1765-4

ORIGINAL PAPER

Structural characterization of the $(MeSH)_4$ potential energy surface

Sara Gómez · Doris Guerra · Jorge David · Albeiro Restrepo

Received: 23 April 2012 / Accepted: 10 January 2013 / Published online: 12 February 2013

Abstract A random walk on the PES for $(MeSH)_4$ clusters produced 50 structural isomers held together by hydrogen-bonding networks according to calculations performed at the B3LYP/6–311++G** and MP2/6–311++G** levels. The geometric motifs observed are somewhat similar to those encountered for the methanol tetramer, but the interactions responsible for cluster stabilization are quite different in origin. Cluster stabilization is not related to the number of hydrogen bonds. Two distinct, well-defined types of hydrogen bonds scattered over a wide range of distances are predicted.

Keywords Stochastic optimization · Hydrogen bonding · Weak interactions · Methanethiol

Introduction

The thiol bond (S–H) is a deceptively simple functional group that plays important roles in biology and chemistry. Thiol bonds, which are present in several amino acids such as cysteine, are thought to contribute to the stabilization of the tertiary and quaternary structures of proteins and biomolecules. Methanethiol (CH_3SH, MeSH) is a colorless gas with an unpleasant odor that is naturally found in living tissues and in physiological environments such as blood and the brain. Methanethiol is a product of the bacterial and metabolic decomposition of proteins and foods that is ultimately eliminated in animal excrement; it is also among the chemical substances responsible for bad breath and other foul odors. Methanethiol is used in a variety of industrial processes, such as those used in the production of animal food and the plastic and pesticide industries, as well as in airplane fuel mixtures; more commonly, because of its strong smell provides warnings against leaks, MeSH is included as an additive in natural gas. The adsorption of methanethiol on several metallic surfaces has been studied [1, 2].

Because oxygen and sulfur atoms have different sizes, electronegativities, and electronic structures, sulfur-containing compounds behave in a chemically different manner to their oxygen-containing analogs. This is especially true in relation to the study reported in the present paper, in which the ability of methanethiol to form stable clusters via hydrogen-bonding networks was investigated. Chemical systems bonded via hydrogen bonds are the subject of intense research, but many aspects of hydrogen bonding remain unclear [3], probably due in part to the difficulties involved in accurately treating the complex energy decomposition schemes associated with such interactions [4].

In this work, we attempt to characterize the potential energy surface (PES) for $(MeSH)_4$ clusters in order to improve the currently limited understanding of this very important PES and to contribute to the field of weakly interacting hydrogen-bonded systems. It is important to recognize that the amount of experimental and theoretical work needed to perform a complete structural characterization of potential energy surfaces as complex as that of $(MeSH)_4$ renders this aspiration impractical. Conformational spaces for weakly hydrogen-bonded systems are notoriously difficult to characterize because of the existence of several complex competing interactions, which can lead to very flat PESs with the presence of possibly numerous shallow local minima. A

Electronic supplementary material The online version of this article (doi:10.1007/s00894-013-1765-4) contains supplementary material, which is available to authorized users.

S. Gómez · D. Guerra · A. Restrepo (✉)
Grupo de Química–Física Teórica, Instituto de Química,
Universidad de Antioquia, AA 1226,
Medellín, Colombia
e-mail: albeiro@matematicas.udea.edu.co

J. David
Escuela de Ciencias y Humanidades,
Departamento de Ciencias básicas,
Universidad Eafit, AA 3300,
Medellín, Colombia

problematic issue in the study of atomic and molecular clusters is the generation of equilibrium structures. Modern advances in technology have produced fast and powerful computers that have allowed the recent implementation of stochastic optimization methods in which the energy is evaluated via quantum Hamiltonians [5–9]. In particular, a modified Metropolis acceptance test in the simulated annealing optimization procedure [10–12] has recently been proposed [13–15] as a means of generating cluster candidate structures that undergo further optimization via traditional gradient-following techniques. This method, incorporated into the ASCEC (Annealing Simulado Con Energía Cuántica) program [15], retains the comparative advantages and disadvantages of stochastic optimization over analytical methods [16] (initial guess independence, exhaustive exploration of the potential energy surface, and the ability to jump over energy barriers and to sample several energy wells in the same run without getting trapped in local minima); however, the method is still computationally intensive due to repetitive evaluation of the energy function. The ASCEC method has been successfully used to treat mono and bimetallic atomic microclusters [14, 17–19], molecular clusters that are linked together via hydrogen-bonding networks [13, 20–24], and mixed atoms/molecules clusters [25] that are stabilized via a wide variety of complex interactions. The studies in question highlighted new structures that had never been reported in the literature before, helping to rationalize bonding in metallic clusters, the stabilization of small hydrogen–bonded networks, the reactivity of metallic microclusters, and the nature of the complex interplay between the forces involved in the microsolvation of alkali metal cations.

Computer methods

We used the molecular cluster capabilities of the ASCEC program [15], which contains a modified Metropolis acceptance test in an adapted version of the simulated annealing optimization procedure. The annealing algorithm [10–12] was used to generate candidate structures after random walks of the PM3 PES. The hybrid B3LYP density functional [26–28] was used in conjunction with the 6–311++G** basis set to optimize and characterize the structures afforded by ASCEC. In order to ensure better treatment of electron correlation and an improved description of the dispersive forces that are probably involved in the stabilization of the title clusters, and due to the extremely high computational demands, we reoptimized only the eight most stable structures at the MP2/6–311++G** level; this subset of structures should be representative of the tendencies in energies and geometries across the entire conformational space. Our choice of model chemistry has proven very accurate for the treatment of hydrogen-bonded clusters [13, 20–24]. Analytical harmonic second-derivative calculations were used to characterize all stationary points as true minima (no negative eigenvalues of the Hessian matrix). Highly correlated CCSD(T)/6–311++G** energies were calculated for all B3LYP- and MP2-optimized geometries. Total binding energies (BE) were calculated by subtracting the energy of a given cluster from the sum of the energies of its constituting moieties. Relative binding energies (ΔBE) were calculated as the difference between the energy of the most stable structure and the energy of a particular cluster on a given PES. All binding and relative energies were corrected for zero-point vibrational energy. All optimization, frequency, and energy calculations were carried out using the Gaussian 03 suite of programs [29]. Isomer populations were estimated by performing standard Boltzmann distribution analysis.

Results and discussion

ASCEC conditions

We used the "big bang" approach to construct the initial geometries for all ASCEC runs: all methanethiol molecules

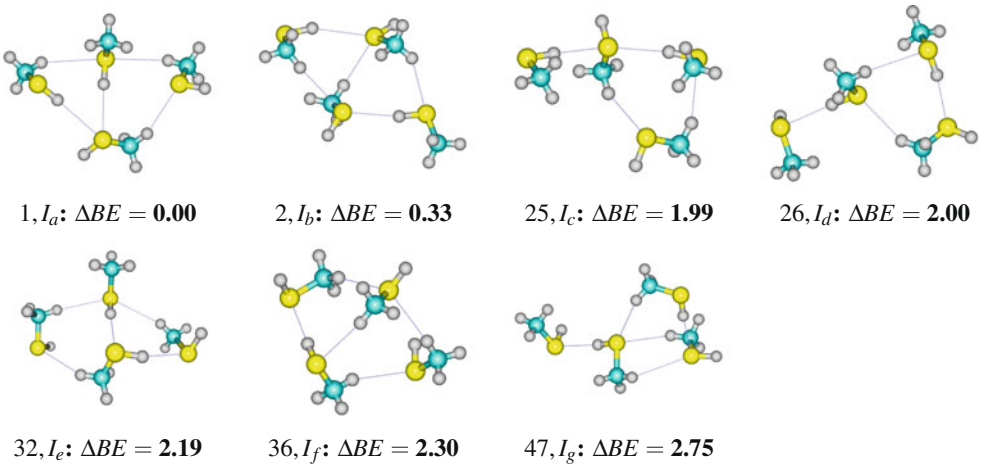

Fig. 1 Group I. The defining geometrical motif includes a five-sided ring with one primary hydrogen bond, two secondary hydrogen bonds, and two formal C–S bonds. The two most stable structures belong to this group. All relative energies are in kcal mol^{-1}, and were calculated at the CCSD(T)/6–311++G**//B3LYP/6–311++G** level

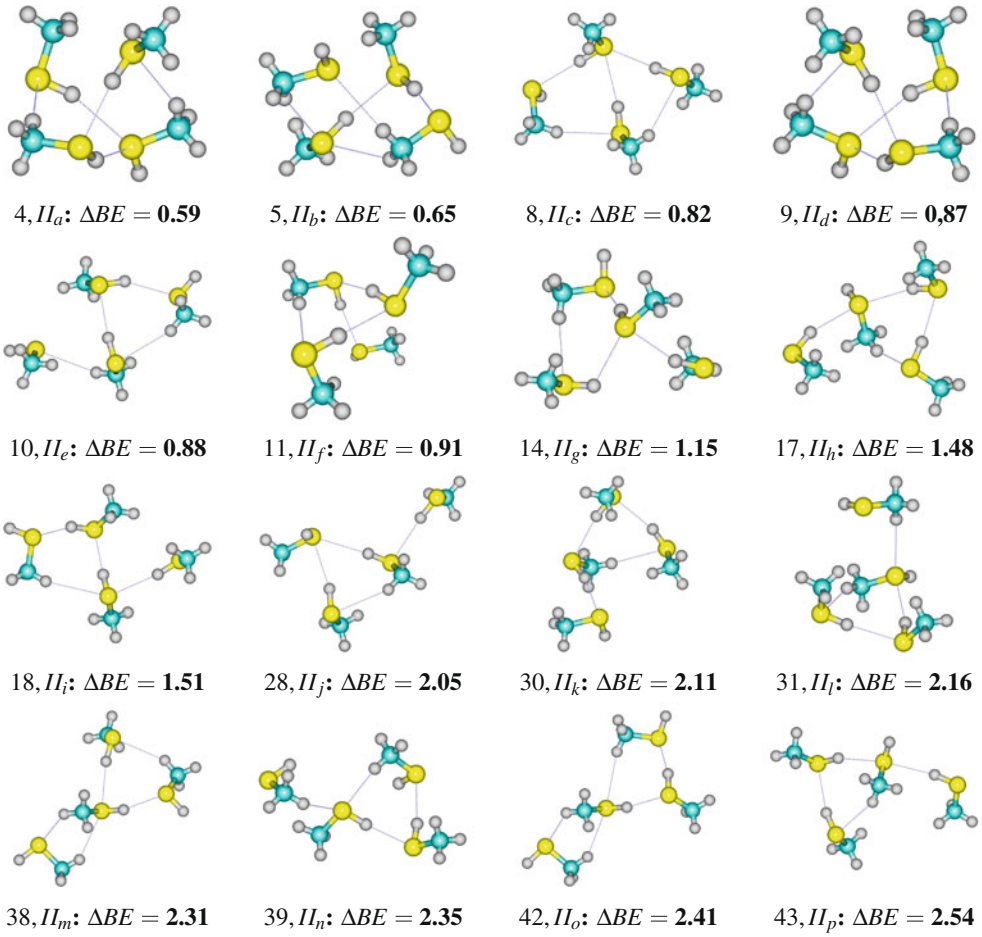

Fig. 2 Group II. The defining geometrical motif includes two consecutive primary hydrogen bonds, a secondary hydrogen bond, and a formal C–S bond. All relative energies are in kcal mol^{-1}, and were calculated at the CCSD(T)/6–311++G**//B3LYP/6–311++G** level

were placed at the same position, and they were allowed to evolve under the annealing conditions within a cube 10 Å on a side. The PM3 semiempirical Hamiltonian was used to calculate the energies of randomly generated cluster configurations; we used geometric quenching routes with initial temperatures of 500 K, a constant temperature decrease of 5 %, and 300 temperatures in total. The stochastic sampling generated 122 candidate structures.

Geometric and structural issues

Equilibrium geometries for the $(CH_3SH)_4$ clusters were produced via the procedure outlined above. The structures, notation, and relative energies within each PES are shown in Figs. 1, 2, 3, 4, 5, 6, 7, 8 and 9. All geometry optimizations were carried out without imposing symmetry constraints, as the structures obtained from ASCEC were randomly generated and belonged to the C_1 point group; however, some of the stationary points located had higher effective (heavy-atom) symmetries.

We found 50 equilibrium structures in the B3LYP/6–311++g** PES, which could be categorized into eight different geometrical motifs, as shown in Figs. 1–9 and listed in Table 1 in approximate decreasing order of stability according to the calculated CCSD(T)/6–311++G**//B3LYP/6–311++G** relative energies. Note that our classification is arbitrary, as chains and other patterns fit into our groups; also, some

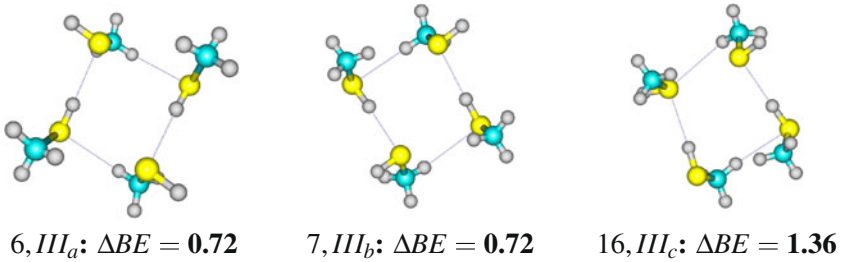

Fig. 3 Group III. The defining geometrical motif includes alternating pairs of primary hydrogen bonds, secondary hydrogen bonds, and formal C–S bonds. All relative energies are in kcal mol^{-1}, and were calculated at the CCSD(T)/6–311++G**//B3LYP/6–311++G** level

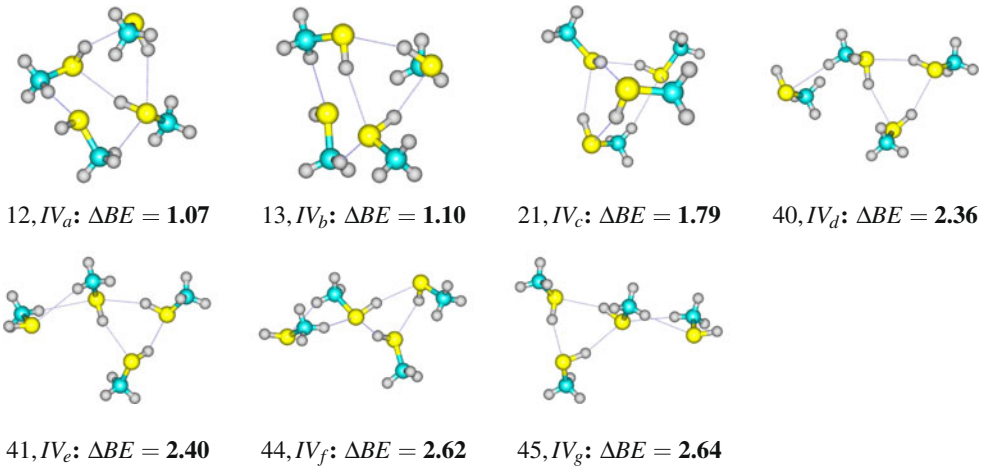

Fig. 4 Group IV. A planar network of three primary hydrogen bonds (a trimer) interacting with an extra MeSH molecule defines this group. All relative energies are in kcal mol^{-1}, and were calculated at the CCSD(T)/6–311++G**// B3LYP/6–311++G** level

structures could belong to more than one group because several motifs may be present in the same cluster. Five structures that do not exhibit any of the eight geometrical motifs were collected into an additional group termed "others." MP2 optimization of the most stable B3LYP structures, which were actually found in four different groups, led to minimal structural deformation and to exactly the same hydrogen-bonding networks that kept the clusters stable.

We decided not to refer to the 50 structures using conventional descriptive methods because this could lead to confusion considering the large number of isomers involved; instead, the eight groups are described by common structural features. Two criteria were used: global relative stability (**1**, **2**, …, **50**; where **1** is the most stable) and the relative stability within each group (I_a, I_b, …, $VIII_b$; where I_a being the most stable in group I, etc.). There are plenty of possibilities and probably more structures to be found within each group due to variations in the orientations of the H and CH_3 substituents relative to the geometrical pattern that defines the group.

Brief description of the groups

Group I (Fig. 1) is defined by a five-sided ring with contributions from three different molecules. The ring features one primary (the donated proton comes from an S–H bond) and two secondary (the donated proton comes from a C–H bond) hydrogen bonds as well as two C–S bonds. Two of the molecules contribute with one secondary bond and one C–S bond each, meaning that their respective SH hydrogens are free of interactions or are used to bond with the fourth methanethiol. There are seven structures in this group.

Group II (Fig. 2) displays a four-sided cyclic pattern with contributions from three molecules, the remaining CH_3SH molecule positioning itself in several different ways around the defining geometrical motif. The cycle contains one secondary and two primary hydrogen bonds in addition to one C–S bond, with one molecule affording the secondary bond, the C–S bond, leaving its own SH hydrogen free from cluster interactions. Sixteen structures were located in this group.

Group III (Fig. 3) features a six-membered ring with alternating C–S, primary, and secondary hydrogen bonds. There are always two SH hydrogens that do not participate in the stabilizing network. There are three structures in this group.

Group IV (Fig. 4) is characterized by a planar network of three primary hydrogen bonds (a trimer) interacting with an extra methanethiol molecule. There are a total of seven structures in this group.

Group V (Fig. 5) contains two structures defined by a six-membered ring with two secondary hydrogen bonds and two C–S bonds. The molecules that participate in C–S bonds leave their own SH hydrogens free from cluster interactions.

Group VI (Fig. 6) contains three stable structures. The geometric pattern that defines the group is a planar network of four primary hydrogen bonds with the methyl groups located above and under the plane. No secondary bonds are present in this group.

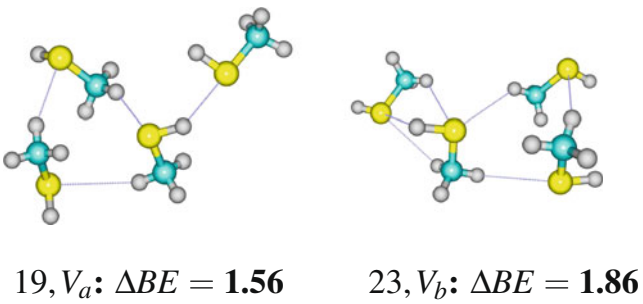

Fig. 5 Group V. The geometrical pattern defining this group is a six-membered ring with alternating C–S and secondary hydrogen bonds. All relative energies are in kcal mol^{-1}, and were calculated at the CCSD(T)/6–311++G**//B3LYP/6–311++G** level

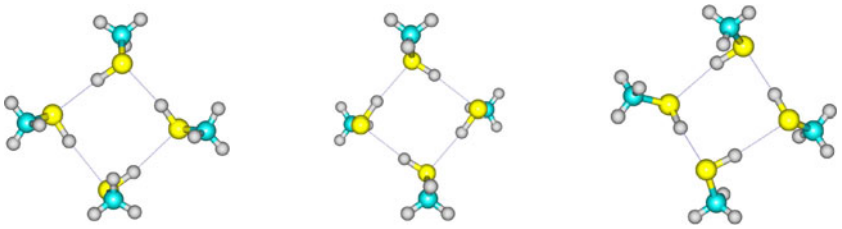

Fig. 6 Group VI. A planar network of four primary hydrogen bonds defines this group; the methyl groups are located above and under the plane. All relative energies are in kcal mol^{-1}, and were calculated at the CCSD(T)/6–311++G**//B3LYP/6–311++G** level

Group VII (Fig. 7) exhibits a five-sided ring to which the four methanethiol molecules contribute. There are three primary and one secondary hydrogen bond in the ring. The fifth side of the ring is afforded by a C–S bond in one of the methanethiol molecules, which is the one that contributes the secondary bond, always leaving its own SH hydrogen free from cluster bonding. We located five structures in this group.

Group VIII (Fig. 8) displays two structures. There are two primary hydrogen bonds in a six-membered cycle, which also contains two secondary hydrogen bonds and two C–S bonds.

Others (Fig. 9) comprises five structures whose geometrical features prevent them from being included in any of the other eight groups. The structures exhibit several degrees of geometric complexity and include the two least stable conformations in the overall order as well as the third most stable isomer.

Primary hydrogen bonds, secondary hydrogen bonds, or combinations of both are involved in bonding to one or more of the molecules that define the geometrical motif when there is an extra molecule. Except for groups I and IV, the defining cycles are often nonplanar. There are many instances of sulfur atoms acting as double acceptors of primary, secondary, or both kinds of hydrogen bonds.

Secondary hydrogen bonds in the clusters are predicted to be≈18 % longer on average than primary bonds. The smallest and largest S···H lengths of a primary hydrogen bond are, respectively, 2.64 and 3.07 Å (2.85 Å average, $r_{max} - r_{min} = 0.43$ Å), while, for secondary bonds, those lengths are 3.03 and 3.70 Å (3.37 Å average, $r_{max} - r_{min} = 0.67$ Å; ratio of the averages= 1.18). Plots of the distributions of the S···H distances for primary and secondary hydrogen bonds are included in Fig. 10. The distributions of S···H distances for primary and secondary hydrogen bonds resemble Gaussian functions centered at the respective average values; the wider range of values seen for secondary bonds makes for a wide variety of possibilities, leading to a rich conformational space.

It has been suggested [30]—and shown in several cases—that for linear hydrogen bonds, the distance from the proton to the center of the hydrogen bond, q_1, correlates quadratically with the distance between the heavy atoms, q_2, with q_1=0 corresponding to a scenario where the proton is shared equally

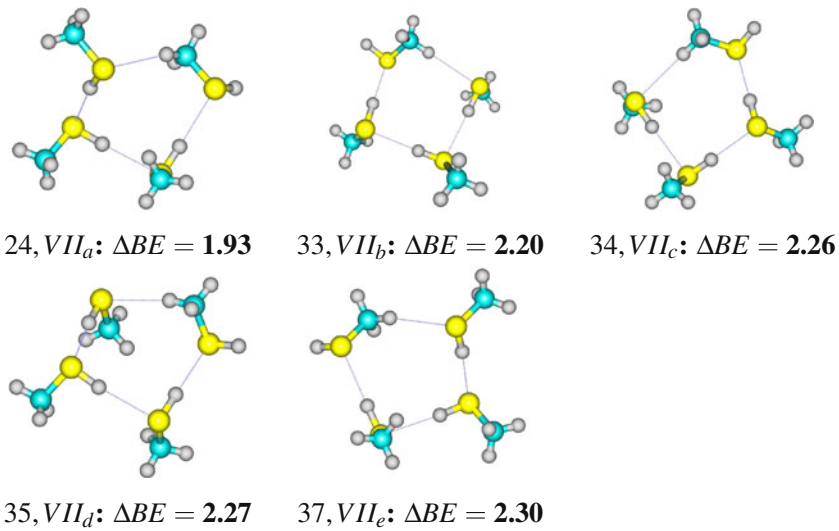

Fig. 7 Group VII. The defining geometrical motif includes three consecutive primary hydrogen bonds, a secondary hydrogen bond, and a formal C–S bond. All relative energies are in kcal mol^{-1}, and were calculated at the CCSD(T)/6–311++G**//B3LYP/6–311++G** level

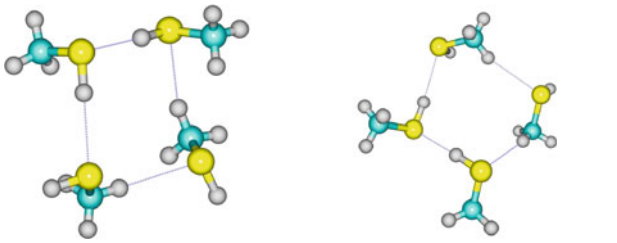

$29, VIII_a$: $\Delta BE = \mathbf{2.09}$ $48, VIII_b$: $\Delta BE = \mathbf{2.85}$

Fig. 8 Group VIII. A common pattern of a nonplanar six-membered ring with two primary and two secondary hydrogen bonds together with two C–S bonds defines this group. All relative energies are in kcal mol^{-1}, and were calculated at the CCSD(T)/6–311++G**//B3LYP/6–311++G** level

between the two heavy atoms (i.e., this is the midpoint for hydrogen transfer). Despite the fact that the hydrogen bonds examined in this work are generally not linear, there is a remarkable quadratic correlation between q_1 and q_2, as depicted in Fig. 11. Fitting the relationship of q_1 to q_2 for primary hydrogen bonds yields the adjusted equation $q_2 = 2.8486 - 1.6854q_1 + 0.1636q_1^2$. This equation reveals that for the $(MeSH)_4$ clusters, every H atom involved in a primary hydrogen bond remains strongly attached to the methanethiol molecule that donates it: the smallest predicted q_2 is 4.05 Å, which is considerably larger than 2.85 Å, the distance corresponding to a proton shared equally between two sulfur atoms (q_1=0). Fitting the relationship of q_1 to q_2 for secondary hydrogen bonds produced the adjusted equation $q_2 = 2.1900 - 1.9838q_1 + 0.0054q_1^2$, and the smallest predicted q_2 is 4.15 Å, which is considerably larger than 2.19 Å, the distance corresponding to a proton shared equally between two sulfur atoms (q_1=0). These observations lead us to suggest that proton transfer in the $(MeSH)_4$ clusters is not favored. More importantly, from Fig. 10, it is clear seen that primary and secondary hydrogen bonds have different physical origins, as there are two separate, well-defined trend lines.

The rich potential energy surface obtained in this study is a consequence of the stochastic nature of the search of the quantum conformational space performed by the ASCEC method [13, 14], which bypasses the structure-guessing step in the search for local minima. The high diversity of structures obtained is due to the presence of the secondary hydrogen bonds, which increase the conformational possibilities: in contrast, water tetramers held together exclusively by primary hydrogen bonds exhibit three geometrical motifs and eight structures [13]. A remarkable finding is that, due to the spatial orientation of the entire cluster, we identified several pairs of enantiomers, even though the cluster does not have a chiral center.

Energetics, cluster stabilization, and other properties

Table 1 lists the clusters in decreasing order of stability as predicted by the CCSD(T)/6–311++G**//B3LYP/6–311++G** calculations. Table 1 also shows their binding energies (BE) and relative binding energies (ΔBE), as calculated at the B3LYP and CCSD(T)//B3LYP levels. Isomer populations, estimated via standard Boltzmann distribution analysis, are also included in Table 1. Table 2 shows analogous results for the MP2 and CCSD(T)//MP2 calculations. Note the extensive overlap between groups and how similar the binding energies are, which means that several isomers have significant populations at standard conditions.

Stability does not seem to depend directly on the number of primary hydrogen bonds, as in the cases of hydrogen-bonding networks involving O–H groups; in the present case, structures with four primary bonds are not the most stable ones. The total number of hydrogen bonds does not correlate with stability either. For example, the most stable structure (**1**, I_a, Fig. 1, Table 1) exhibits two primary and three secondary

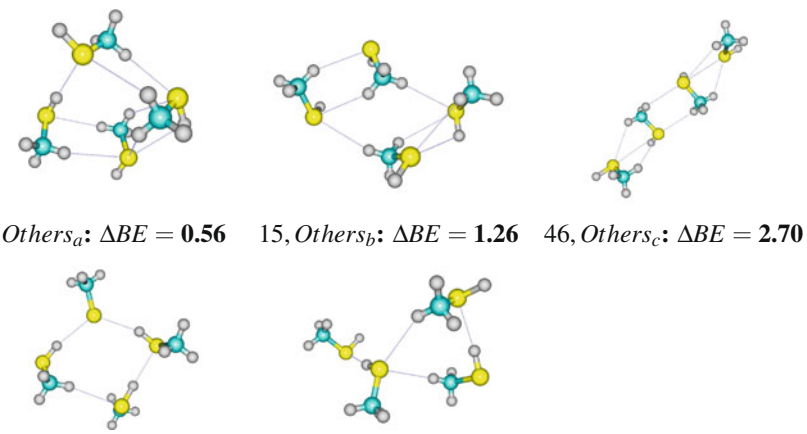

$3, Others_a$: $\Delta BE = \mathbf{0.56}$ $15, Others_b$: $\Delta BE = \mathbf{1.26}$ $46, Others_c$: $\Delta BE = \mathbf{2.70}$

$49, Others_d$: $\Delta BE = \mathbf{3.32}$ $50, Others_e$: $\Delta BE = \mathbf{3.55}$

Fig. 9 Group "others." The structures belonging to this group did not have any characteristics in common, and were also unrelated to any of the other groups. All relative energies are in kcal mol^{-1}, and were calculated at the CCSD(T)/6–311++G**//B3LYP/6–311++G** level

Table 1 B3LYP and CCSD(T)//B3LYP binding (BE) and relative binding (ΔBE) energies for $(MeSH)_4$ (all energies are in kcal mol^{-1}; $\%x_i$ are the estimated Boltzmann populations at 298 K; all calculations were performed using the 6–311++G** basis set)

Order	Structure	BE [B3LYP]	ΔBE [B3LYP]	BE [CCSD(T)]	ΔBE [CCSD(T)]	$\%x_i$
1	I_a	2.93	2.24	10.49	0.00	18.02
2	I_b	2.78	2.40	10.16	0.33	9.61
3	$Others_a$	2.82	2.35	9.93	0.56	6.32
4	II_a	3.77	1.40	9.90	0.59	6.32
5	II_b	3.73	1.44	9.84	0.65	5.13
6	III_a	3.55	1.62	9.78	0.72	5.13
7	III_b	3.55	1.62	9.77	0.72	5.13
8	II_c	3.51	1.66	9.67	0.82	4.16
9	II_d	3.77	1.40	9.40	0.87	4.16
10	II_e	3.51	1.67	9.61	0.88	4.16
11	II_f	3.99	1.18	9.58	0.91	3.37
12	IV_a	3.70	1.48	9.42	1.07	2.73
13	IV_b	3.77	1.40	9.40	1.10	2.73
14	II_g	3.11	2.06	9.34	1.15	2.22
15	$Others_b$	1.72	3.45	9.23	1.26	2.22
16	III_c	3.09	2.09	9.13	1.36	1.80
17	II_h	3.60	1.57	9.02	1.48	1.46
18	II_i	3.86	1.31	8.98	1.51	1.46
19	V_a	1.92	3.26	8.93	1.56	1.18
20	VI_a	4.67	0.60	8.74	1.76	0.96
21	IV_c	3.78	1.39	8.71	1.79	0.78
22	VI_b	5.17	0.00	8.66	1.83	0.78
23	V_b	2.08	3.09	8.64	1.86	0.78
24	VII_a	4.09	1.08	8.56	1.93	0.63
25	I_c	3.10	2.07	8.50	1.99	0.63
26	I_d	2.99	2.18	8.49	2.00	0.63
27	VI_c	4.65	0.52	8.45	2.04	0.51
28	II_j	2.90	2.27	8.44	2.05	0.51
29	$VIII_a$	3.21	1.96	8.41	2.09	0.51
30	II_k	3.39	1.79	8.38	2.11	0.51
31	II_l	2.95	2.22	8.33	2.16	0.41
32	I_e	3.42	1.76	8.30	2.19	0.41
33	VII_b	4.31	0.87	8.29	2.20	0.41
34	VII_c	4.31	0.86	8.23	2.26	0.41
35	VII_d	3.82	1.35	8.22	2.27	0.34
36	I_f	2.67	2.50	8.19	2.30	0.34
37	VII_e	4.06	1.11	8.20	2.30	0.34
38	II_m	3.23	1.94	8.18	2.31	0.34
39	II_n	3.41	1.77	8.14	2.35	0.34
40	IV_d	3.51	1.66	8.13	2.36	0.34
41	IV_e	3.38	1.79	8.09	2.40	0.27
42	II_o	3.19	1.98	8.08	2.41	0.27
43	II_p	3.38	1.79	7.95	2.54	0.22
44	IV_f	3.31	1.86	7.87	2.62	0.22
45	IV_g	3.34	1.84	7.85	2.64	0.22
46	$Others_c$	2.22	2.95	7.80	2.70	0.18
47	I_g	2.67	2.51	7.74	2.75	0.18
48	$VIII_b$	3.43	1.75	7.64	2.85	0.15
49	$Others_d$	3.00	2.17	7.17	3.32	0.06
50	$Others_e$	2.51	2.67	6.94	3.55	0.04

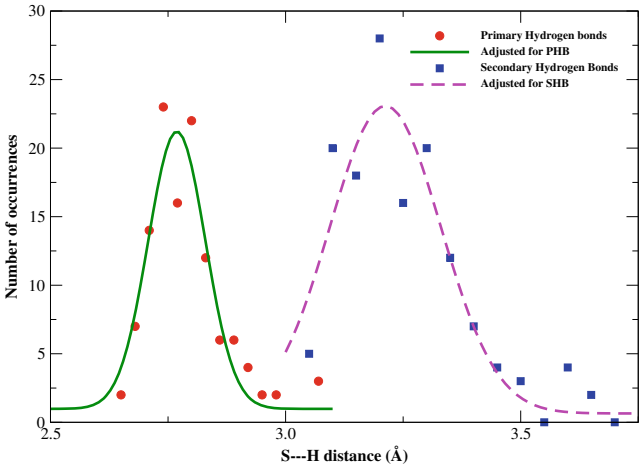

Fig. 10 Distribution of S···H distances for primary and secondary hydrogen bonds in the methanethiol tetramers. Data taken from the B3LYP/6–311++G** optimized geometries

hydrogen bonds, while structure number **12** in the stability order (IV_a, Fig. 4, Table 1) shows three primary and two secondary hydrogen bonds.

As opposed to hydrogen-bonded networks involving O–H groups, cluster stabilization in $(MeSH)_4$ cannot be understood by invoking the joint effect of cooperative polarization and cooperative charge transfer. For the methanol tetramer, the most closely related system, the most stable structures are those found in group VI for $(MeSH)_4$; this is additional evidence that the forces governing methanol cluster stabilization—which are thought to include dominant contributions from electrostatic interactions [20]—are very different to those involved in the stabilization of methanethiol clusters. This can be rationalized in terms of the higher electronegativity of the oxygen atom when compared to the sulfur atom,

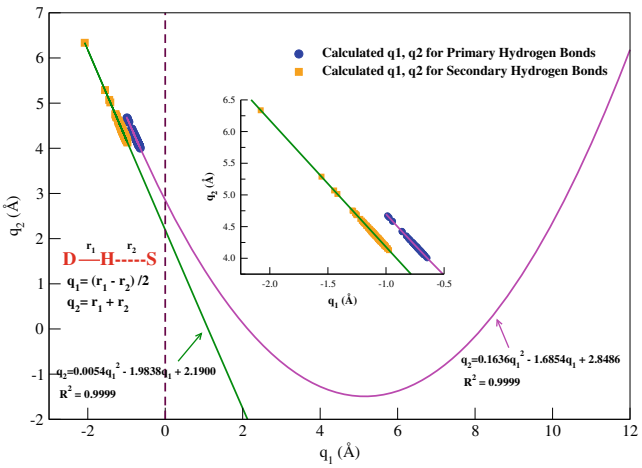

Fig. 11 Correlation between q_2, the approximate distance between donor and acceptor atoms, and q_1, the approximate distance from the proton to the center of the hydrogen bond

Table 2 MP2 and CCSD(T)//MP2 binding (BE) and relative binding (ΔBE) energies for $(MeSH)_4$ (all energies are in kcal mol^{-1}; all calculations were performed using the 6–311++G** basis set)

Order	Structure	BE [MP2]	*ΔBE* [MP2]	BE [CCSD(T)]	*ΔBE* [CCSD(T)]
1	I_a	12.95	0.18	14.41	0.13
2	I_b	12.51	0.61	13.90	0.63
3	$Others_a$	12.87	0.25	14.54	0.00
4	II_a	12.57	0.56	13.93	0.60
5	II_b	13.04	0.09	14.40	0.14
6	III_a	13.12	0.00	14.37	0.17
7	III_b	13.12	0.00	14.38	0.16
8	II_c	12.05	1.07	13.52	1.07

which yields highly polar O–H bonds, meaning that electrostatic interactions are major players in the stabilization of O–H hydrogen-bonding networks [13, 20–24]. Additional evidence of the relative weakness of the interactions responsible for stabilization in $(MeSH)_4$ clusters when compared to $(MeOH)_4$ is the smaller stabilization energies, which lead to excessive mixing of the structures in the groups, as already pointed out (19–37 kcal mol^{-1} in $(MeOH)_4$ [20] vs. 7–10 kcal mol^{-1} for $(MeSH)_4$, Table 1). It was also found that B3LYP performs remarkably well in the prediction of molecular geometries because most methanol tetramer structures are reproduced for the methanethiol tetramers and because, upon MP2 refinement of the geometries, the clusters undergo minimal structural changes while retaining the stabilizing hydrogen-bonding networks. However, B3LYP does a rather poor job of predicting binding and relative energies, as seen when comparing CCSD(T)//B3LYP and CCSD(T)//MP2 against pure B3LYP binding energies (Tables 1 and 2). Tables 1 and 2 show that high levels of electron correlation are needed to properly calculate binding energies because B3LYP underestimates and MP2 overestimates energy quantities; however, and perhaps more importantly, CCSD(T) energy differences remain in the same 0–1 kcal mol^{-1} range, regardless of the method used to optimize the cluster geometries.

Conclusions and perspectives

We report the geometries and properties of 50 structural isomers located on the PES of (methanethiol)$_4$. The structures were found after a random walk on the PES subject to a modified Metropolis acceptance test produced 122 candidates. The isomers were categorized into eight geometric motifs. Two distinct types of hydrogen bonds were observed: primary hydrogen bonds (in which an S–H group acts as proton donor) and secondary hydrogen bonds (in which the donated proton comes from a C–H bond). Cluster

stabilization is not related to the total number of hydrogen bonds nor to the number of primary hydrogen bonds. The geometric motifs are somewhat similar to those encountered for the methanol tetramer, but the interactions responsible for cluster stabilization are quite different in origin. Weak interactions led to a very complex PES with hydrogen bonds covering a wide range of distances. B3LYP did a good job of predicting molecular geometries, but accurate calculations of interaction energies required the use of highly correlated CCSD(T) methods. The results in this study by no means provide a complete characterization of the PES, as there are probably more structures to be located due to the many conformational possibilities afforded by the presence of secondary hydrogen bonds.

Acknowledgments Financial support from Universidad de Antioquia, Comite para el desarrollo de la investigacion (CODI) office, is acknowledged. Partial funding by Universidad EAFIT (internal project number 261–00002) is also acknowledged.

References

1. Wang L, Tsymbal E, Jaswal S (2004) Phys Rev B 70:075410
2. Saavedra M, Buljan A, Muñoz M (2009) J Mol Struc (THEOCHEM) 906:72
3. Masella M, Gresh N, Flament J (1998) J Chem Soc 94:2745
4. Koch W, Holthausen M (2002) Hydrogen bonds and weakly bound systems. In: A chemist's guide to density functional theory, 2nd edn. Wiley, New York
5. Alexandrova A, Boldyrev A (2005) J Chem Theory Comput 1:566
6. Jellinek J, Srinivas S, Fantucci P (1998) Chem Phys Lett 288:705
7. Bazterra V, Oña O, Caputo M, Ferraro M, Fuentealba P, Facelli J (2004) J Phys Rev A 69:053202
8. Tiznado W, Oña O, Bazterra V, Caputo M, Facelli J, Ferraro M, Fuentealba P (2005) J Chem Phys 123:214302
9. Oña O, Bazterra V, Caputo M, Facelli J, Fuentealba P, Ferraro M (2006) Phys Rev A 73:053203
10. Metropolis N, Rosenbluth A, Rosenbluth M, Teller A, Teller E (1953) J Chem Phys 21:1087
11. Kirkpatrick S, Gellat C, Vecchi M (1983) Science 220:671
12. Aarts E, Laarhoven H (1987) Simulated annealing: theory and applications. Springer, New York
13. Pérez J, Hadad C, Restrepo A (2008) Int J Quantum Chem 108:1653
14. Pérez J, Flórez E, Hadad C, Fuentealba P, Restrepo A (2008) J Phys Chem A 112:5749
15. Pérez J, Restrepo A (2008) ASCEC V–02: Annealing Simulado con Energía Cuántica. Property, development and implementation. Grupo de Química–Física Teórica, Instituto de Química, Universidad de Antioquia, Medellín
16. Restrepo A, Mari F, Gonzalez C, Marquez M (1995) Química, Actualidad y Futuro 5:101
17. David J, Guerra D, Restrepo A (2012) Chem Phys Lett 539–540:64
18. Yepes D, Kirk S, Jenkins S, Restrepo A (2012) J Mol Mod 18:4171
19. David J, Guerra D, Hadad C, Restrepo A (2010) J Phys Chem A 114:10726
20. David J, Guerra D, Restrepo A (2009) J Phys Chem A 113:10167
21. Murillo J, David J, Restrepo A (2010) Phys Chem Chem Phys 12:10963
22. Hincapié G, Acelas N, Castaño M, David J, Restrepo A (2010) J Phys Chem A 114:7809
23. Ramírez F, Hadad C, Guerra D, David J, Restrepo A (2011) Chem Phys Lett 507:229
24. Jenkins S, Restrepo A, David J, Yin D, Kirk S (2011) Phys Chem Chem Phys 13:11644
25. Romero J, Reyes A, David J, Restrepo A (2011) Phys Chem Chem Phys 13:15264
26. Stephens P, Devlin J, Chabalowski C, Frisch M (1994) J Phys Chem 98:11623
27. Lee C, Yang W, Parr R (1988) Phys Rev B 37:785
28. Becke A (1993) J Chem Phys 98:5648
29. Frisch MJ, Trucks GW, Schlegel HB, Scuseria GE, Robb MA, Cheeseman JR, Montgomery Jr JA, Vreven T, Kudin KN, Burant JC, Millam JM, Iyengar SS, Tomasi J, Barone V, Mennucci B, Cossi M, Scalmani G, Rega N, Petersson GA, Nakatsuji H, Hada M, Ehara M, Toyota K, Fukuda R, Hasegawa J, Ishida M, Nakajima T, Honda Y, Kitao O, Nakai H, Klene M, Li X, Knox JE, Hratchian HP, Cross JB, Bakken V, Adamo C, Jaramillo J, Gomperts R, Stratmann RE, Yazyev O, Austin AJ, Cammi R, Pomelli C, Ochterski JW, Ayala PY, Morokuma K, Voth GA, Salvador P, Dannenberg JJ, Zakrzewski VG, Dapprich S, Daniels AD, Strain MC, Farkas O, Malick DK, Rabuck AD, Raghavachari K, Foresman JB, Ortiz JV, Cui Q, Baboul AG, Clifford S, Cioslowski J, Stefanov BB, Liu G, Liashenko A, Piskorz P, Komaromi I, Martin RL, Fox DJ, Keith T, Al–Laham MA, Peng CY, Nanayakkara A, Challacombe M, Gill PMW, Johnson B, Chen W, Wong MW, Gonzalez C, Pople JA (2004) Gaussian 03, revision E.01. Gaussian, Inc., Wallingford
30. Limbach H, Tolstoy P, Pérez-Hernández N, Gou J, Shemderovich J, Denisvo G (2009) Isr J Chem 49:199